Many-body physics in two-component Bose-Einstein condensates in a cavity: fragmented superradiance and polarization

Axel Lode, Fritz Diorico, Rugway Wu, Paolo Molignini, Luca Papariello, Rui Lin, Camille Lévêque, Lukas Exl, Marios Tsatsos, R Chitra, et al.

PAPER • OPEN ACCESS

Many-body physics in two-component Bose–Einstein condensates in a cavity: fragmented superradiance and polarization

To cite this article: Axel U J Lode *et al* 2018 *New J. Phys.* **20** 055006

New Journal of Physics
The open access journal at the forefront of physics

Deutsche Physikalische Gesellschaft DPG
IOP Institute of Physics

Published in partnership with: Deutsche Physikalische Gesellschaft and the Institute of Physics

OPEN ACCESS

RECEIVED
8 January 2018

REVISED
7 March 2018

ACCEPTED FOR PUBLICATION
6 April 2018

PUBLISHED
15 May 2018

PAPER

Many-body physics in two-component Bose–Einstein condensates in a cavity: fragmented superradiance and polarization

Axel U J Lode[1,2,7], Fritz S Diorico[2], RuGway Wu[2], Paolo Molignini[3], Luca Papariello[3], Rui Lin[3], Camille Lévêque[1,2], Lukas Exl[4,5], Marios C Tsatsos[6], R Chitra[3] and Norbert J Mauser[1]

[1] Wolfgang Pauli Institute c/o Faculty of Mathematics, University of Vienna, Oskar-Morgenstern Platz 1, A-1090 Vienna, Austria
[2] Vienna Center for Quantum Science and Technology, Atominstitut, TU Wien, Stadionallee 2, A-1020 Vienna, Austria
[3] Institute for Theoretical Physics, ETH Zurich, 8093 Zurich, Switzerland
[4] Faculty of Mathematics, University of Vienna, Oskar-Morgenstern Platz 1, A-1090 Vienna, Austria
[5] Institute for Analysis and Scientific Computing, Vienna University of Technology, Wiedner Hauptstraße 8-10, A-1040 Wien, Austria
[6] São Carlos Institute of Physics, University of São Paulo, PO Box 369, 13560-970 São Carlos, São Paulo, Brazil
[7] Author to whom any correspondence should be addressed.

E-mail: axel.lode@univie.ac.at

Keywords: many-body systems, time-dependent Schrödinger equation, Bose–Einstein condensates, light–matter interaction, multi-component systems, MCTDHB

Abstract

We consider laser-pumped one-dimensional two-component bosons in a parabolic trap embedded in a high-finesse optical cavity. Above a threshold pump power, the photons that populate the cavity modify the effective atom trap and mediate a coupling between the two components of the Bose–Einstein condensate. We calculate the ground state of the laser-pumped system and find different stages of self-organization depending on the power of the laser. The modified potential and the laser-mediated coupling between the atomic components give rise to rich many-body physics: an increase of the pump power triggers a self-organization of the atoms while an even larger pump power causes correlations between the self-organized atoms—the BEC becomes fragmented and the reduced density matrix acquires multiple macroscopic eigenvalues. In this fragmented superradiant state, the atoms can no longer be described as two-level systems and the mapping of the system to the Dicke model breaks down.

1. Introduction

Cavity quantum electrodynamics (QED) is a burgeoning field of research due to recent rapid technological progress in the fields of optics, electronics and optoelectronic devices. From scalable quantum computers [1–4] to controlling atoms in an ultracold atomic ensemble [5, 6], atoms coupled to light in cavities have opened promising new avenues of research. In particular, due to the ability to precisely control and manipulate ultracold atoms, trapped ultracold atoms in optical cavities have emerged as a prime choice for simulating cavity QED [7]. The paradigmatic light–matter Dicke phase transition was first realized using cold atoms in [8] and subsequently, other setups [9–11] have simulated the Dicke model [12].

The impact of realizing such models goes beyond the field of ultracold atoms. Namely, cavity QED provides hybrid quantum systems [13–17] that are one route to storing quantum information with long decoherence times. Indeed, ultracold atoms are readily accessible and can have decoherence times of several seconds [15, 18]; thus ultracold atoms and, in particular, their hyperfine states (usually the 'clock states') have bright prospects for quantum information storage. Attempts to collectively couple the microwave hyperfine ground state of an ultracold atomic ensemble in a cavity QED setting with a superconducting resonator are already being pursued by numerous groups across the world despite the substantial technical challenges [19–24].

In recent years cavity QED experiments with ultracold atoms in optical cavities have evolved substantially [25, 26]. In this work, we take a first step towards understanding the physics of two-component trapped one-dimensional (1D) ultracold atoms incorporating interparticle interactions as well as coupling to a cavity. Our results extend the understanding of experimental control of multi-component systems through optical cavities.

Interestingly, cavity QED can also be used to mediate interactions between atoms within an ultracold atomic ensemble [10]. In the dispersive regime, a transverse pump beam is coupled to the longitudinal atomic motion of the ultracold atoms. The atomic motion, in turn, may populate the cavity modes via photons scattered by the moving atoms. Thus, depending on the pump power, a self-organization of the atomic density is triggered [10, 27]. It is possible to resonantly control these interactions: in a spinor, two- or multi-component condensate, the atomic states can be coupled with each other via an optical [7] or a microwave cavity [19, 24].

Theoretically, cavity QED can be described by the Tavis–Cummings Hamiltonian or generally the Dicke model [12, 28, 29]. The representation of ultracold atoms in an optical cavity by the Dicke model involves a simplification which is justified as long as the atomic ensemble is appropriately modeled by a two-level system. However, in a degenerate ultracold ensemble, the atoms are moving and interacting, and the Dicke model may thus breakdown [30, 31].

For single- and multi-component BECs, i.e., BECs of atoms with internal degrees of freedom, the basic model is the Gross–Pitaevskii equation. It is an approximation that incorporates interactions through a specific mean-field approximation based on the expectation value of the bosonic field and, as such, neglects correlations [32–34]. The inclusion of atom–atom scattering together with atom-cavity coupling is, however, likely to affect the correlations between the atoms: the back-action of the photons onto the atomic state can be cast in the form of a cavity-mediated optical lattice. Non-trivial correlations are known to emerge between cold atoms, in optical lattices, for example the superfluid-Mott transition in the Bose–Hubbard model [35, 36], and are beyond the realm of mean-field theories; such correlations thus entail many-body effects that cannot be described by the Gross–Pitaevskii model. The original proposal [19] to couple ultracold atoms to a superconducting microwave cavity, for instance, neglected the interparticle interactions and thereby the interesting correlations that emerge in 1D multi-component condensates [37].

A representative example for a many-body effect is the so-called *fragmentation* [38, 39] of the BEC. Fragmentation can be quantified using the reduced one-body density matrix (RDM); if the RDM has only a single macroscopic eigenvalue the system is said to be condensed [40], while if the RDM has more than one macroscopic eigenvalue the state is said to be fragmented [38, 39, 41, 42–55]. Fragmentation has been recently demonstrated to emerge in single-component ultracold bosons coupled to a single-mode cavity for pump powers roughly four times as large as the pump power necessary to drive the system from the normal to the superradiant phase [30]. Importantly, fragmentation and consequently correlations are also known to be present in spinor condensates [37, 56–59].

We study the many-body physics of a 1D two-component BEC in a high-finesse optical cavity as a function of the power of the applied transversal laser pumps, see figure 1. We consider a setup where the photons that populate the cavity mode through Raman scattering modify the one-body potential of the atoms and mediate a coupling between the two components of the BEC, see also [60]. We go beyond [60] and exploit the capabilities of the multiconfigurational time-dependent Hartree method for indistunguishable particles X (MCTDH-X) [37, 61–63] to accurately [64–66] include interactions and correlations between the atoms trapped by an external confinement. Reference [60] studies two-component bosons without an external potential and with no interactions, i.e., a system in which a discrete $\mathbf{Z}_2$ symmetry is present and may be broken spontaneously. Our investigation below deals with confined and interacting bosons, i.e., a more realistic system where correlations play a crucial role and the discrete $\mathbf{Z}_2$ symmetry is absent. Our results thus *complement* the findings in [60].

To this end, we extended the MCTDH-X software [63] to interacting bosons with internal structure [37] that are coupled to an optical cavity. To cast the evolution of the cavity field amplitude in the form of a partial differential equation, we introduce a complex damping term that describes the cavity losses phenomenologically and circumvents the necessity to solve a complicated master equation. This approximation is particularly good for the experimental setup considered in the paper where $\Delta_c \gg \Delta_a$ and it is compatible with adiabatic elimination. We use MCTDH-X to find the ground states and investigate the density, momentum density, the effective potential, fragmentation, cavity population, and polarization (i.e. the fraction of atoms in each component) of the ground state as a function of the strength of the pumps.

We find that the combined system of atoms and photons undergoes two transitions. For moderate pump powers the atoms self-organize; the system is described by the Dicke model and exhibits a transition from a normal to a superradiant phase. For larger pump powers in the superradiant phase, the reduced one-body density matrix of the atoms acquires several macroscopic eigenvalues—the BEC fragments and the combined system of light and matter enters the fragmented superradiant phase [30]. Together with this second transition, an almost complete polarization of the atoms emerges and, simultaneously, the two-level description of the atomic ensemble—and therewith the Dicke model—breaks down.

This paper is structured as follows. In section 2 we introduce the Hamiltonian, the quantities of interest and the method used. In section 3 we describe our results on the many-body physics of ultracold interacting two-component bosons with cavity-mediated coupling between the components. A short discussion and outlook follow in section 4.

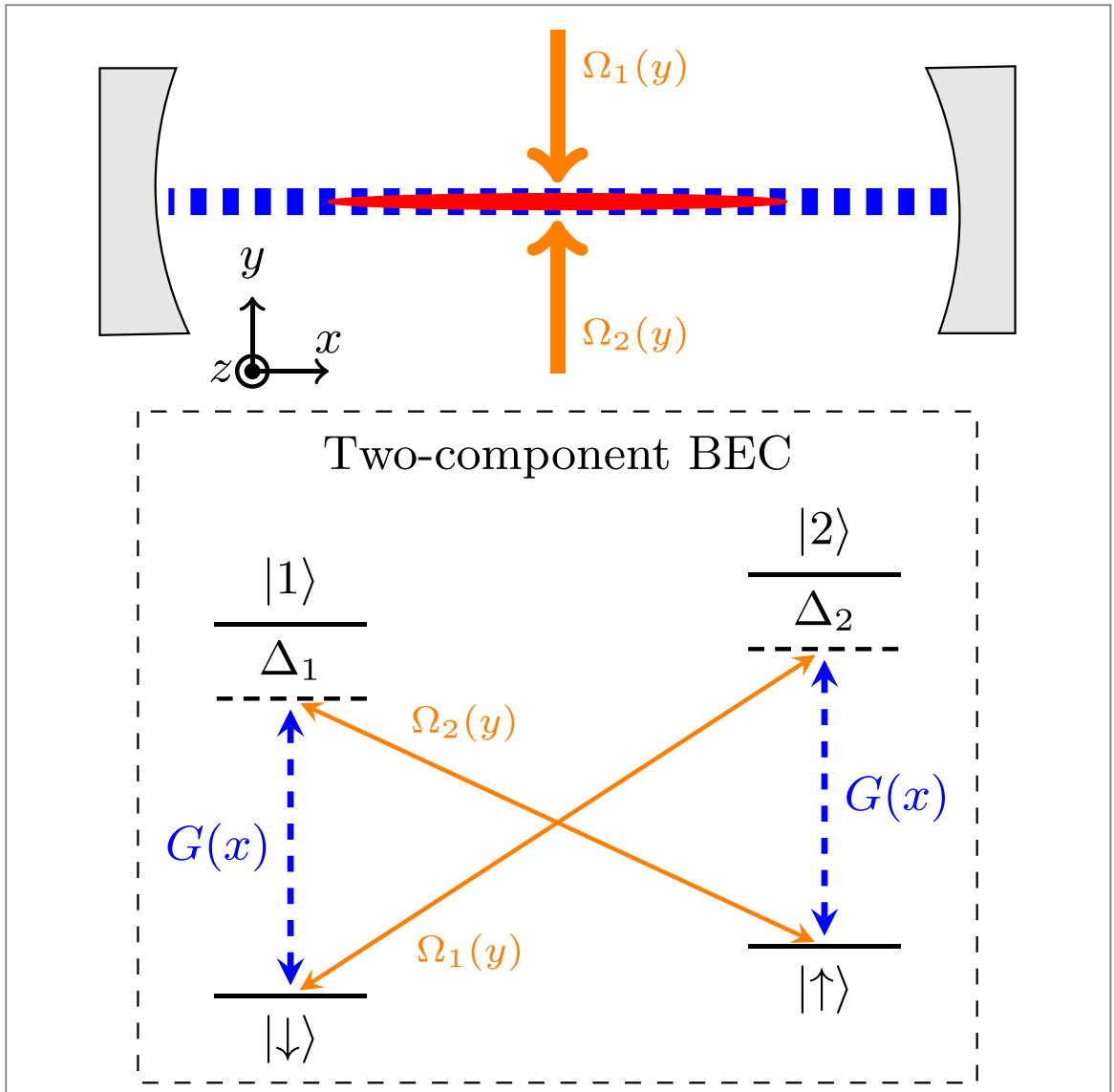

Figure 1. One-dimensional two-component quasi-condensate in a high-finesse optical cavity. The ultracold two-component bosons are pumped by two transverse pump beams that couple to the transitions between the atomic states $|\downarrow\rangle$ and $|2\rangle$ and between $|\uparrow\rangle$ and $|1\rangle$ with Rabi frequencies Ω_1 and Ω_2, respectively (see dashed box). The coupling to the cavity is given by $G(x) = g_0 \cos(k_c x)$ for both transitions, where g_0 is the single atom coupling strength, see text. In the self-organized phase, the cavity mode is populated (blue dashes) and acts on the atoms as a potential and effective coupling between the $\uparrow$ and $\downarrow$ component.

2. System and method

The time-dependent 1D many-boson Schrödinger equation in dimensionless units[8] is

$$\hat{H}|\Psi\rangle = \mathrm{i}\partial_t|\Psi\rangle. \tag{1}$$

Here, $|\Psi\rangle$ is the many-body wavefunction of N bosons in M single-particle states

$$|\Psi\rangle = \sum_{\vec{n}=(n_1,\ldots,n_M)} C_{\vec{n}}(t) \prod_{k=1}^{M} \left[\frac{(\hat{b}_k^\dagger)^{n_k}}{\sqrt{n_k!}}\right]|\mathrm{vac}\rangle, \tag{2}$$

where, $\hat{b}_k^\dagger$ is the bosonic creation operator acting on the vacuum $|\mathrm{vac}\rangle$, n_k is the occupation of the kth single-particle state and $C_{\vec{n}}(t)$ is a time-dependent coefficient. The sum in equation (2) runs over all configurations $\vec{n} = (n_1, \ldots, n_M)$ with a fixed number of particles $n_1 + \cdots + n_M = N$. Here and in the following we use

[8] To arrive at the dimensionless units, we divide the Hamiltonian by $\frac{\hbar^2}{mL^2}$. To arrive at the interaction parameters $\lambda_0^\uparrow = 0.0975$ and $\lambda_0^\downarrow = 0.1$, we first fix a length scale of $L = 1$ μm. The scale of energy for the mass m of ^{87}Rb is $\hbar^2/(mL^2) = 116$ Hz and the scale of time is $mL^2/\hbar = 1.37$ ms. According to [67], the 1D scattering lengths λ are the three-dimensional scattering lengths a_{3D} rescaled by the frequency $\omega_\perp$ of the transversal confinement by $\lambda = 2Lm\omega_\perp a_{3D}/\hbar$. We pick the $\xi = \uparrow$ state and map $\lambda_0^\uparrow$ to $a_{3D}^{11} = 100.4a_0$, where a_0 is the Bohr radius. One obtains $\omega_\perp = \lambda_0\hbar/(2Lma_{3D}^{11}) = 687.9$ Hz.

dimensionless units (see footnote 8 on page 3) obtained by dividing the many-body Hamiltonian by $\frac{\hbar^2}{mL^2}$ where m is the mass of the particles and L the unit of length. Atomic losses are neglected in this work.

Since the bosons have two components the single-particle states $\vec{\varphi}_k^*(x;\,t)$ associated with the creation operators $\hat{b}_k^\dagger$ are mutually orthonormal vectors,

$$\vec{\varphi}_k^*(x;\,t) = \sum_{\xi=\uparrow,\downarrow} \phi_k^{\xi,*}(x;\,t)\,\mathbf{1}^\xi, \tag{3}$$

made up of two functions $\phi_k^{\xi,*}$. Here $\mathbf{1}^\xi$ denotes the unit vector in the space of components. In the following we use the term 'components' to refer to the contribution of the $\phi_k^\uparrow(x;\,t)$ and $\phi_k^\downarrow(x;\,t)$ functions to the many-body state $|\Psi\rangle$, while we use the terms 'orbitals' or 'single-particle states' to refer to the vectors $\vec{\varphi}_k(x;\,t)$, respectively.

The position-space Hamiltonian of the ultracold system of two-component bosons coupled to the cavity reads

$$\hat{H} = \sum_{i=1}^{N} \hat{\underline{h}}(x_i;\,t) + \sum_{i<j=1}^{N} \hat{\underline{W}}(x_i,\,x_j;\,t). \tag{4}$$

Here, $\hat{\underline{h}}(x;\,t)$ is the one-body operator that contains the kinetic energy, the confinement potential $\underline{V}(x,\,t)$, and a cavity-mediated term $\underline{V}^{\text{cavity}}(x,\,t)$, i.e.,

$$\begin{aligned}\hat{\underline{h}}(x;\,t) &= \left[-\frac{1}{2}\partial_x^2 + \underline{V}(x,\,t)\right] + \underline{V}^{\text{cavity}}(x,\,t)\\ &= \sum_{\xi=\uparrow,\downarrow}\left[-\frac{1}{2}\partial_x^2 + V_\xi(x,\,t)\right]\mathbf{1}^\xi\mathbf{1}^{\xi,T} + \underline{V}^{\text{cavity}}(x,\,t).\end{aligned} \tag{5}$$

The action of the cavity photons on the atoms is given by the one-body potential $\underline{V}^{\text{cavity}}(x)$:

$$\underline{V}^{\text{cavity}}(x) = \begin{pmatrix} V_{\uparrow\uparrow}^{\text{cavity}}(x) & V_{\uparrow\downarrow}^{\text{cavity}}(x) \\ V_{\downarrow\uparrow}^{\text{cavity}}(x) & V_{\downarrow\downarrow}^{\text{cavity}}(x)\end{pmatrix}. \tag{6}$$

The diagonal terms $V_{\uparrow\uparrow}^{\text{cavity}}$, $V_{\downarrow\downarrow}^{\text{cavity}}$ prescribe a modification of the one-body confinement V_ξ, while the off-diagonal ones, $V_{\downarrow\uparrow}^{\text{cavity}}$, $V_{\uparrow\downarrow}^{\text{cavity}}$, induce a cavity-mediated coupling between the components [60]:

$$\begin{aligned} V_{\uparrow\uparrow}^{\text{cavity}}(x) &= U_\uparrow|\alpha|^2\cos^2(k_c x),\\ V_{\downarrow\downarrow}^{\text{cavity}}(x) &= U_\downarrow|\alpha|^2\cos^2(k_c x) + \tilde{\delta},\\ V_{\uparrow\downarrow}^{\text{cavity}}(x) = V_{\downarrow\uparrow}^{\text{cavity}}(x) &= \eta(\alpha + \alpha^*)\cos(k_c x).\end{aligned} \tag{7}$$

The parameters $U_{\uparrow,\downarrow}|\alpha|^2$ describe the depths of the cavity-mediated optical lattices for the two components, with k_c and $\tilde{\delta}$ being the wave vector of the cavity mode and the offset between the two optical lattices, respectively. The cavity pump power η governs the coupling between different components. The parameters $U_{\uparrow,\downarrow}$ are determined by the dipole matrix elements and the detuning.

The cavity field amplitude α is given by the following equation of motion [30, 60]:

$$\begin{aligned}\mathrm{i}\partial_t\alpha(t) = &\left[-\Delta_c + \sum_{k,q=1}^{M}(\rho_{kq}(t)\,U_{kq}(t)) - \mathrm{i}\kappa\right]\alpha(t)\\ &+ \sum_{k,q=1}^{M}(\rho_{kq}(t)\eta_{kq}(t)),\end{aligned} \tag{8}$$

where $\rho_{kq}(t) = \langle\Psi(t)|\hat{b}_k^\dagger\hat{b}_q|\Psi(t)\rangle$ are the matrix elements of the RDM, Δ_c is the detuning of the cavity frequency with respect to the laser pump, and the decay rate κ accounts for photons leaking out of the cavity. Here, we also introduced the matrix elements

$$U_{kq} = \langle\vec{\varphi}_k|\sum_{\xi=\uparrow,\downarrow}\mathbf{1}^\xi\mathbf{1}^{\xi,T}U_\xi|\alpha|^2\cos^2(k_c x)|\vec{\varphi}_q\rangle, \tag{9}$$

$$\begin{aligned}\eta_{kq} &= \langle\vec{\varphi}_k|\eta\cos(k_c x)\begin{pmatrix}0 & 1\\ 1 & 0\end{pmatrix}|\vec{\varphi}_q\rangle\\ &= \eta\int\mathrm{d}x(\cos(k_c x)[\phi_k^{\uparrow,*}(x)\phi_q^\downarrow(x) + \phi_k^{\downarrow,*}(x)\phi_q^\uparrow(x)]).\end{aligned} \tag{10}$$

The U_{kq} matrix elements define the back-action of individual atomic components on the cavity field amplitude α. The elements η_{kq} define a coupled back-action of both atomic components on the cavity field amplitude α and are zero for polarized atoms.

We note that the single distinction of the mathematical framework for the description of microwave cavities as opposed to optical cavities is the magnitude of the cavity wave vector k_c: for microwave cavities, the $\cos(k_c x)$ terms in equations (7), (9), (10) could be considered constants.

To complete our mathematical description, we consider an identical parabolic confinement for both components of the atomic cloud,

$$V_\uparrow(x) \equiv V_\downarrow(x) = \frac{1}{2}x^2, \tag{11}$$

and contact interparticle interactions of atoms within the same component,

$$\underline{\hat{W}}(x, x') = \sum_{\xi=\uparrow,\downarrow} (\mathbf{1}^\xi \mathbf{1}^{\xi,T} \lambda_0^\xi \delta(x - x')). \tag{12}$$

We fix the interaction strength to be weakly repulsive and slightly different for each component: for the $\uparrow$ component, we set $\lambda_0^\uparrow = 0.0975$ and for the $\downarrow$ component $\lambda_0^\downarrow = 0.1$ in dimensionless units; see footnote 8 on page 3 for a dimensionalized model using ^{87}Rb atoms. Since the interactions in the $\uparrow$ component are slightly weaker, a larger population in the $\uparrow$ state is energetically favorable. Note that, for simplicity, we have neglected interparticle interactions of atoms in distinct components that are present in ultracold spinor bosons [37, 68].

In this paper, we use the multiconfigurational time-dependent Hartree method for indistinguishable particles software [63] to solve equation (1) for the many-body ground state. To that end, the time-dependent variational principle is used to derive a set of equations of motion for both the coefficients and the single-particle states entering the multiconfigurational ansatz in equation (2). Optimizing both the coefficients and the single-particle states ensures that the relevant part of the many-body Hilbert space is spanned efficiently. Here, we consider a system of $N = 100$ atoms described by $M = 3$ single-particle states coupled to equation (8) for the population of photons in the cavity.

To compute the ground state, we propagate the coupled equations (1) and (8) in imaginary time to damp out all excited states. Note that the populations of the different components are varying in the process of imaginary time propagation, as the excitations of the system may have a different atom numbers in the components. The obtained ground state distributions of atoms between components are such that the total energy of the system is minimized.

We remark that we work in dimensionless units throughout by dividing the many-body Hamiltonian by $\frac{\hbar^2}{mL^2}$ where m is the mass of the considered particles and L the unit of length. For example with ^{87}Rb atoms and $L \equiv 1\ \mu$m, the longitudinal extent of the system we consider is roughly 4–6 μm yielding roughly 15–20 atoms per micron (see footnote 8 on page 3). Furthermore, atomic losses are neglected in this work.

We investigate a cavity with parameters related to Esslinger's experimental setup with an optical cavity [8] and consider a two-component system with two transversal pumps and the coupling scheme illustrated in figure 1, see also [60]. The pumps and the cavity are far-red-detuned from the atomic transition. We define the atomic and cavity detunings $\Delta_{1/2}$ and Δ_c, in terms of the energies of the involved states $|1\rangle$, $|2\rangle$, $|\uparrow\rangle$, $|\downarrow\rangle$, respectively, $E_{|1\rangle} = \hbar\omega_1$, $E_{|2\rangle} = \hbar\omega_2$, $E_{|\uparrow\rangle} = \hbar\omega_\uparrow$, $E_{|\downarrow\rangle} = \hbar\omega_\downarrow$. We fix $E_{|\downarrow\rangle} \equiv 0$ and obtain the detunings:

$$\begin{aligned}
\Delta_1 &= \frac{\omega_{\Omega_1} + \omega_{\Omega_2}}{2} - \omega_1, \\
\Delta_2 &= \omega_{\Omega_2} - \omega_2, \\
\Delta_c &= \frac{\omega_{\Omega_1} + \omega_{\Omega_2}}{2} - \omega_c.
\end{aligned}$$

We assume that these atomic detunings are large enough compared to the kinetic energy in the excited states $|1\rangle$, $|2\rangle$ such that we can eliminate them from our description, see [60] for details. We consider two-photon Raman transitions to be close to-resonant, i.e., $\omega_\uparrow \approx \omega_c - \omega_{\Omega_1} \approx \omega_{\Omega_2} - \omega_c$. The relative two-photon detuning is $\delta = \omega_\uparrow - \frac{\omega_{\Omega_2} - \omega_{\Omega_1}}{2}$. The coupling of the $|\downarrow\rangle$($|\uparrow\rangle$)-component to the atomic excited state $|1\rangle$ ($|2\rangle$) is $G(x) = g_0 \cos(k_c x)$. The cavity pump power is $\eta = \frac{g_0\Omega_1}{\Delta_1} = \frac{g_0\Omega_2}{\Delta_2}$, the cavity detuning is $\Delta_C = -42992$, the cavity loss-rate $\kappa = 5555$, the k-vector of the cavity $k_c = 4.9$, the cavity-atom coupling $U_\downarrow = \frac{g_0^2}{\Delta_1} = 1$, $U_\uparrow = \frac{g_0^2}{\Delta_2} = 2$, and the potential offset $\tilde{\delta} = \delta + \frac{\Omega_1^2}{\Delta_1} - \frac{\Omega_2^2}{\Delta_2}$ is a Stark-shifted two-photon detuning [60].

In dimensionalized units (see footnote 8 on page 3), we have $(\Delta_c, \kappa, U_\uparrow, U_\downarrow) = (-2\pi \times 4.987$ MHz, $2\pi \times 0.6444$ MHz, 1457.7 Hz, 728.849 Hz).

3. Polarization and fragmentation of two-component bosons in a cavity

We now discuss the physics of the ground state of the two-component BEC as a function of the cavity pump power. As quantities of interest, we use the reduced one-body density matrix $\boldsymbol{\rho}^{(1)}(x, x') = \langle\Psi|\hat{\Psi}^\dagger(x')\hat{\Psi}(x)|\Psi\rangle$, and its diagonal (simply called density) $\boldsymbol{\rho}(x) \equiv \boldsymbol{\rho}^{(1)}(x, x' = x)$, and the amplitude of the cavity field $|\alpha|$. Since we consider two-component bosons, the densities are also two-component quantities. The quantity $\mathbf{1}^\uparrow\boldsymbol{\rho}(x)$ is the *component density*, as it gives the density of the $\uparrow$ component; likewise for the $\downarrow$ component. The sum of the component densities is the *total* density. Figures 2(a)–(c) show the component densities together and the total density as a function of the pump power η.

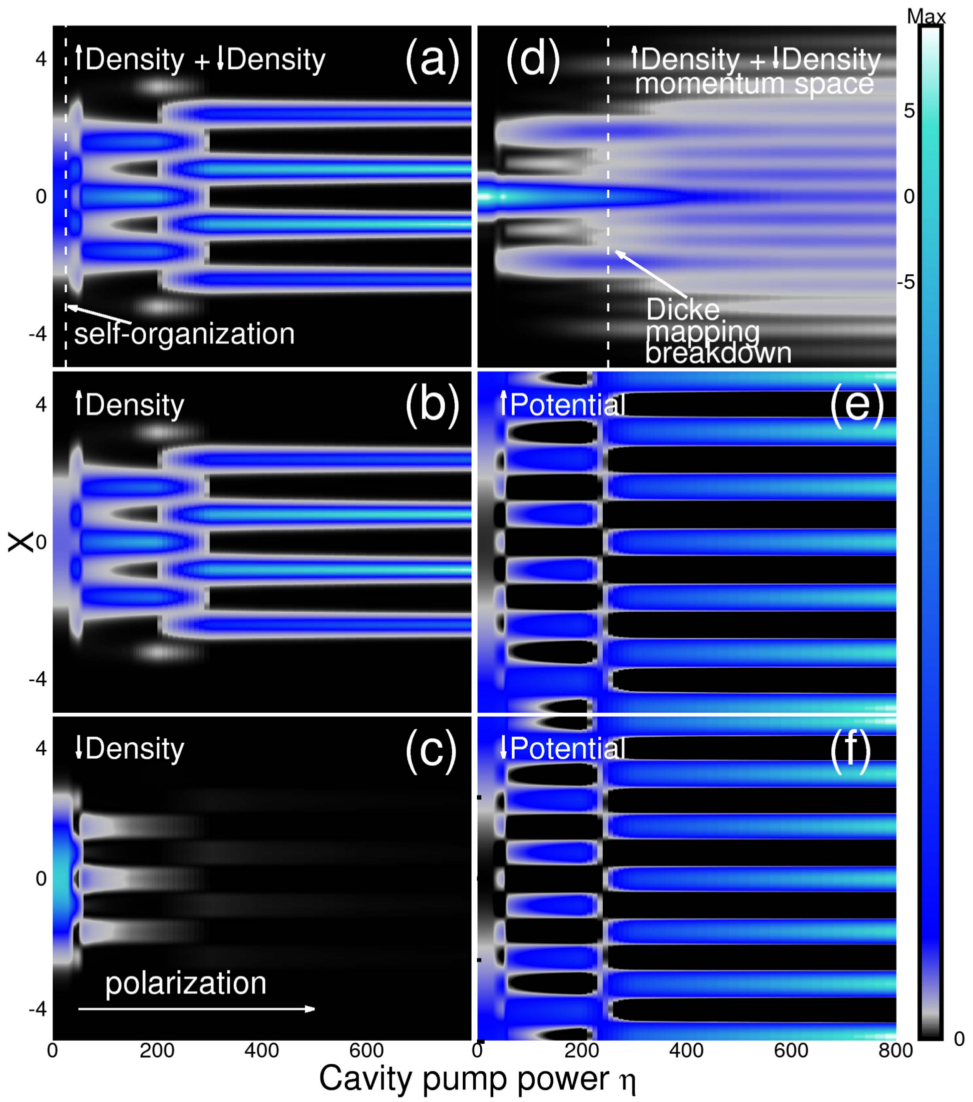

Figure 2. Tracing the self-organization of a two-component Bose–Einstein condensate in a cavity. The total [↑/↓] density (a) (b)/(c), the total momentum density (d), and cavity-modified potential $V_{\uparrow,\downarrow}(x) + V^{\text{cavity}}_{\uparrow\uparrow,\downarrow\downarrow}(x)$ (e)/(f) are depicted as functions of the cavity pump power. The transition to the superradiant state in which the cavity field amplitude is nonzero and the atoms self-organize happens at $\eta_c \approx 25$ (see white dashed line in panel (a)). For larger η, the state becomes polarized (panels (b), (c)) and the ↓ density goes to zero. The density (a)–(c) and potential (e), (f) change the number of humps and minima, respectively, in the superradiant phase. This change happens at the pump powers η where the real and imaginary parts of the cavity field amplitude α (figure 3(a)) change sign. The self-organization of the two-component system results in the formation of peaks at $\pm k_c$ in the total momentum distribution, see panel (d). The emergence of fragmentation leads to the formation of additional structure with a spacing of about $k_c/3$ in the momentum distribution, see vertical dashed line in panel (d). See text for further discussion.

Examining the density and its components, already reveals rich physics: close to zero pump power η each component sees a potential that is almost harmonic as the cavity population α is zero (see figures 2(e)–(f) and 3(a)). The respective densities are therefore Gaussian-shaped and show no spatial modulation (figures 2(a)–(c)). In the mapping of the system to the Dicke model, this absence of spatial modulation corresponds to the normal phase [11, 12]. In the normal phase, the momentum distribution has a maximum at zero with no secondary peak (figure 2(d)).

As the cavity pump power crosses a threshold value of $\eta_c \approx 25$, the cavity field amplitude (figure 3(a)) increases and the atoms self-organize into a periodic structure as a consequence of the cavity-mediated potential (see equation (7)). This self-organization is a hallmark of the transition of the system to the superradiant state of the equivalent Dicke model [11, 12].

With a further increase of the pump power, i.e., $\eta \in [25, 120]$ the atomic ground state becomes polarized in an almost purely ↑-component state due to the cavity-mediated potential and coupling between the components (see equation (7) and figures 2(e), (f)). This polarization can be quantified by the fraction of atoms in the ↑ component,

$$P = \frac{1}{N}\int \mathrm{d}x\,\{\mathbf{1}^{\uparrow}\boldsymbol{\rho}(x)\},$$

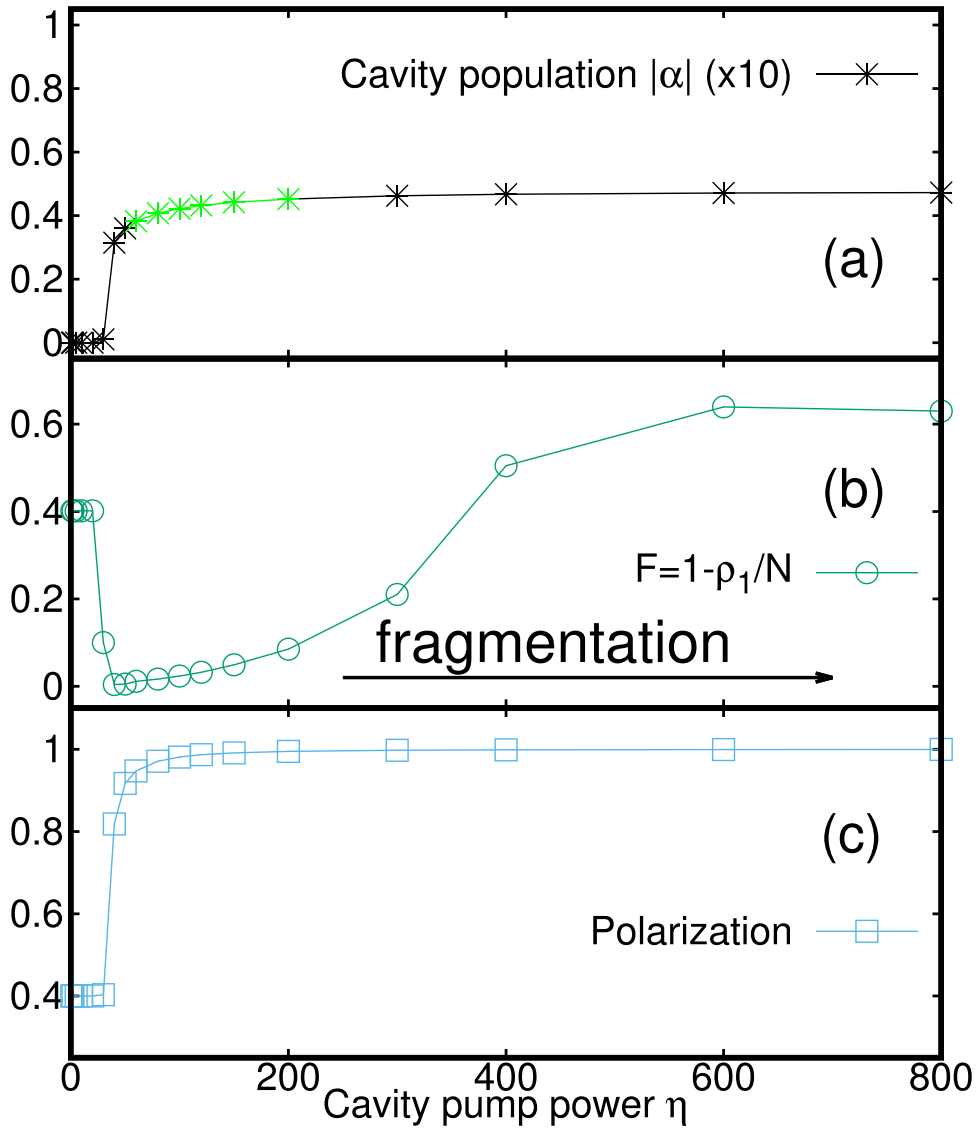

Figure 3. Cavity population, fragmentation, and polarization of two-component bosons in a cavity. At transition to superradiance of the Dicke model equivalent to the cold atoms in the cavity, $\eta \approx 25$, the cavity field amplitude $|\alpha|$ shows a sharp increase (panel (a)). The fragmentation (panel (b)) of the state is quenched from 40% to almost zero at the transition to superradiance. For larger pump powers η, concurrently with the polarization of the atoms (panel (c)), fragmentation re-emerges, however, at a smaller rate. This re-emergence of fragmentation heralds the breakdown of the mapping of the system to the Dicke model (compare momentum density in figure 2(d)). The real and imaginary parts of the cavity field amplitude α (panel (a)) change sign at the pump powers η where the density changes from a two- to a three-hump and from a three- to a four-hump structure in the superradiant phase (see figures 2(a)–(c), (e)–(f)), see green/black (gray/black) part of $|\alpha|$-plot in panel (a) and text for further discussion.

plotted in figure 3(c). At pump powers above $\eta \approx 120$, less than 1% of the atoms are in the $\downarrow$ state. This polarization can be understood as a consequence of the structure of the potential in equation (7); for large pump power η, the contribution of the off-diagonal potential terms, $V^{\text{cavity}}_{\uparrow\downarrow,\downarrow\uparrow}$, to the energy is minimized by polarized states. Since the expectation values of these off-diagonal potential terms always involve an $\uparrow$ and a $\downarrow$ contribution, they vanish if either the $\uparrow$ or the $\downarrow$ component is unpopulated.

The observed self-organization behavior can also be understood as a consequence of the cavity-mediated change of the one-body potential, $V_{\uparrow,\downarrow}(x) + V^{\text{cavity}}_{\uparrow\uparrow,\downarrow\downarrow}(x)$: the density of both components (see figures 2(b) and (c)) is intuitively located at the minima of the potential (see figures 2(e) and (f)).

We now turn to the emergence of correlations in the many-body state; for this purpose, we use the eigenvalues $\{n_k; k = 1, \ldots, M\}$ of the reduced one-body density matrix $\boldsymbol{\rho}^{(1)}(x, x')$. We quantify fragmentation by the fraction F of atoms that does not correspond to the largest eigenvalue n_1:

$$F = \frac{1}{N}\left(\sum_{k=2}^{M} n_k\right) = 1 - \frac{n_1}{N}. \tag{13}$$

The fraction F is 40% at zero pump power, see figure 3(b). This finding is a consequence of the slightly different interaction strengths of each component as well as the offset $\tilde{\delta}$ of the component potentials; if both interaction strengths were set equal and $\tilde{\delta}$ zero, a two-fold fragmented state with $\frac{n_1}{N} = \frac{n_2}{N} \approx 50\%$ would be obtained as the ground state, because this configuration minimizes the contribution of the interactions (see equation (12)) to the total energy.

When the atoms self-organize at $\eta_c \approx 25$ and the Dicke model equivalent to the system becomes superradiant, fragmentation and F are almost zero. For the range $\eta \in [25, 600]$ of larger pump powers, however, fragmentation significantly increases; F is larger than 0.5 above $\eta \approx 400$. The emergence of fragmentation is accompanied by a sharp growth of the atomic polarization. Above a cavity pump power of $\eta \approx 120$, the system is completely polarized and almost all bosons sit in the $\uparrow$ state. The $\uparrow$ component is thus in a fragmented superradiant phase analogous to the one found for a single-component Bose–Einstein condensate in a cavity in [30]. This fragmented superradiant phase goes beyond the two-level physics presupposed in the Dicke model [12] for the single-component case [30].

Since the observed fragmented state in our two-component system is similar to the fragmented superradiant state found in [30], it is of interest to assess the (in)applicability of the Dicke two-level picture for the present two-component case as well. For this purpose, we analyze the momentum density in figure 2(d).

The momentum density clearly demonstrates that the Dicke model whose momentum states are at $k = \pm k_c$ and zero, qualitatively describes the physics of the system only for cavity pump powers η for which fragmentation is essentially absent: the momentum density is essentially a three-humped structure with maxima at $k = \pm k_c$ and zero for pump powers $\eta \lesssim 250$. Here, we omitted the analysis of the component momentum densities because the ground state is almost completely polarized already for pump powers η much smaller than 250.

As the system enters the fragmented superradiant phase for $\eta \gtrsim 250$, the Dicke model becomes inapplicable: we observe the emergence of additional structure with a $\frac{k_c}{3}$-spacing in the momentum density in our simulations in figure 2(d). We verified with an MCTDH-X simulation including $M = 4$ orbitals that the $\frac{k_c}{3}$ spacing is not a feature of the applied approximation. Note that the momentum density corresponds to the *diagonal* of the reduced momentum density matrix $\boldsymbol{\rho}^{(1)}(k, k' = k)$. This is a marked difference between the present and the fragmented superradiant state found for a single-component system in [30]. In the single-component case, the Dicke model also breaks down in the transition to fragmented superradiance; however, a structure with a $\frac{k_c}{2}$-spacing is formed in the *off-diagonal* of the reduced momentum density matrix, $\rho^{(1)}(k, k' = -k)$ while the momentum density $\rho^{(1)}(k, k)$ is Gaussian-shaped.

4. Conclusions and outlook

We have investigated the many-body physics of ultracold laser-pumped two-component bosons in a cavity. Above a first threshold of the pump power, the atoms self-organize and the system enters a superradiant state that is qualitatively described by the Dicke model. When the power of the laser pumps is increased the bosons become polarized. Above the pump power necessary for this polarization, fragmentation and correlations between the atoms emerge gradually: the reduced density matrix of the superradiant atomic ensemble acquires multiple macroscopic eigenvalues and the Bose–Einstein condensate becomes fragmented. A $\frac{k_c}{3}$-spaced pattern in the momentum distribution of the bosons heralds the breakdown of the Dicke model and the transition to a fragmented superradiant state. Our findings can be detected by a straightforward measurement of the atom numbers that populate the components and the momentum density after time-of-flight expansion.

We stress that our study explicitly includes correlations and investigates a system that is a promising candidate for ultracold-based quantum computation [69]. Understanding and possibly controlling correlations triggered in ultracold atoms interfaced with cavities enriches the field with an important contribution towards the generation of a scalable quantum computer. For instance, collision-induced highly entangled cluster states [70–72] can be used as initially prepared resource states to engineer measurement-based one-way quantum computations [73–76]. The scheme considered in this work provides an essential building block in the development of scalable quantum computers involving systems of ultracold atoms [77].

Cavity QED with ultracold atoms is essentially described by the same Hamiltonian for both microwave and optical cavities. For optical cavities, the photon wavelength is smaller than the size of the ultracold cloud. The structure of the cavity mode influences the physics of the system within the optical cavity. Also, the photon recoil is not negligible. For the case of a microwave cavity as proposed in [19], the photon recoil can be neglected, and since the wavelength of microwave radiation is much larger than the typical size of the atomic cloud, the cavity mode does not impose additional non-uniform potential on the atomic ensemble.

We thus applied a many-body theory, the multiconfigurational time-dependent Hartree method for indistunguishable particles X (MCTDH-X), and described different phases and their correlation properties; we demonstrated rich physics that result from an intricate interplay of polarization, self-organization, correlations and fragmentation. To enable a protocol that manages the correlations of the system, further studies are needed to understand the mechanism behind the $\frac{k_c}{3}$-pattern in the momentum distribution as well as the behavior of the emergent effects as a function of the offset δ and the couplings $U_\uparrow$, $U_\downarrow$. Future studies may also include interparticle interactions between atoms in distinct components, multi-modal [78, 79] and microwave [19, 20] cavities, or consider more than one spatial dimension. Furthermore, the non-equilibrium dynamics of self-organization [31] or the investigation of fermionic systems [80] or systems with cavity-mediated long-range [10] and/or dipole–dipole [81, 82] interactions are of exceptional interest.

Acknowledgments

We thank Jörg Schmiedmayer for numerous insightful discussions and comments. We acknowledge financial support by the Austrian Science Foundation (FWF) under grant No. F65 (SFB 'Complexity in PDEs'), grant No. F40 (SFB 'FOQUS'), grant No. F41 (SFB 'ViCoM'), grant No. P 31140-N32 ('ROAM'), and the Wiener Wissenschafts- und TechnologieFonds (WWTF) project No. MA16-066 ('SEQUEX'). We acknowledge financial support from FAPESP, the hospitality of the Wolfgang-Pauli-Institut, computation time on the Hazel Hen cluster of the HLRS in Stuttgart and the HPC2013 cluster, financial support from the Swiss National Science Foundation and Mr G Anderheggen.

References

[1] Giovannetti V, Vitali D, Tombesi P and Ekert A 2000 *Phys. Rev.* A **62** 032306
[2] Kim M D and Kim J 2017 *Quantum Inf. Process.* **16** 192
[3] Wei H-R and Deng F-G 2014 *Sci. Rep.* **4** 7551
[4] Brecht T, Pfaff W, Wang C, Chu Y, Frunzio L, Devoret M H and Schoelkopf R J 2016 *npj Quantum Inf.* **2** 16002
[5] Henschel K, Majer J, Schmiedmayer J and Ritsch H 2010 *Phys. Rev.* A **82** 033810
[6] Henkel C, Powers B and Sols F 2005 *J. Phys.: Conf. Ser.* **19** 34
[7] Brennecke F, Donner T, Ritter S, Bourdel T, Köhl M and Esslinger T 2007 *Nature* **450** 268
[8] Baumann K, Guerlin C, Brennecke F and Esslinger T 2010 *Nature* **464** 1301
[9] Garraway B M 2011 *Phil. Trans. R. Soc.* A **369** 1137
[10] Ritsch H, Domokos P, Brennecke F and Esslinger T 2013 *Rev. Mod. Phys.* **85** 553
[11] Baumann K, Mottl R, Brennecke F and Esslinger T 2011 *Phys. Rev. Lett.* **107** 140402
[12] Dicke R H 1954 *Phys. Rev.* **93** 99
[13] Putz S, Angerer A, Krimer D O, Glattauer R, Munro W J, Rotter S, Schmiedmayer J and Majer J 2017 *Nat. Photon.* **11** 36
[14] Astner T, Nevlacsil S, Peterschofsky N, Angerer A, Rotter S, Putz S, Schmiedmayer J and Majer J 2017 *Phys. Rev. Lett.* **118** 140502
[15] Schoelkopf R J and Girvin S M 2008 *Nature* **451** 664
[16] Berman P (ed) 1994 *Cavity Quantum Electrodynamics* (Boston, MA: Academic)
[17] Kurizki G, Bertet P, Kubo Y, Mølmer K, Petrosyan D, Rabl P and Schmiedmayer J 2015 *Proc. Natl Acad. Sci.* **112** 3866
[18] Deutsch C, Ramirez-Martinez F, Lacroûte C, Reinhard F, Schneider T, Fuchs J N, Piéchon F, Laloë F, Reichel J and Rosenbusch P 2010 *Phys. Rev. Lett.* **105** 020401
[19] Verdú J, Zoubi H, Koller C, Majer J, Ritsch H and Schmiedmayer J 2009 *Phys. Rev. Lett.* **103** 043603
[20] Minniberger S, Diorico F, Haslinger S, Hufnagel C, Novotny C, Lippok N, Majer J, Koller C, Schneider S and Schmiedmayer J 2014 *Appl. Phys.* B **116** 1017
[21] Jessen F *et al* 2014 *Appl. Phys.* B **116** 665
[22] Siercke M, Chan K S, Zhang B, Beian M, Lim M J and Dumke R 2012 *Phys. Rev.* A **85** 041403
[23] Bernon S *et al* 2013 *Nat. Commun.* **4** 2380
[24] Hattermann H, Bothner D, Ley L Y, Ferdinand B, Wiedmaier D, Sárkány L, Kleiner R, Koelle D and Fortágh J 2017 *Nat. Commun.* **8** 2254
[25] Norcia M A, Lewis-Swan R J, Cline J R K, Zhu B, Rey A M and Thompson J K 2017 arXiv:1711.03673
[26] Masson S J, Barrett M D and Parkins S 2017 *Phys. Rev. Lett.* **119** 213601
[27] Brennecke F, Ritter S, Donner T and Esslinger T 2008 *Science* **322** 235
[28] Tavis M and Cummings F W 1968 *Phys. Rev.* **170** 379
[29] Tavis M and Cummings F W 1969 *Phys. Rev.* **188** 692
[30] Lode A U J and Bruder C 2017 *Phys. Rev. Lett.* **118** 013603
[31] Molignini P, Papariello L, Lode A U J and Chitra R 2017 arXiv:1710.02474
[32] Pethick C J and Smith H 2002 *Bose–Einstein Condensation in Dilute Gases* (Cambridge: Cambridge University Press)
[33] Bogoliubov N N 1991 *Selected Works II: Quantum and Statistical Mechanics* (New York: Gordon and Breach)
[34] Pitaevskii L P and Stringari S 2003 *Bose–Einstein Condensation* (Oxford: Clarendon)
[35] Jaksch D, Bruder C, Cirac J I, Gardiner C W and Zoller P 1998 *Phys. Rev. Lett.* **81** 3108
[36] Greiner M, Mandel O, Esslinger T, Hänsch T W and Bloch I 2002 *Nature* **415** 39
[37] Lode A U J 2016 *Phys. Rev.* A **93** 063601
[38] Nozières P and Saint James D 1982 *J. Phys.* **43** 1133
[39] Spekkens R W and Sipe J E 1999 *Phys. Rev.* A **59** 3868
[40] Penrose O and Onsager L 1956 *Phys. Rev.* **104** 576
[41] Streltsov A I, Alon O E and Cederbaum L S 2007 *Phys. Rev. Lett.* **99** 030402

[42] Bader P and Fischer U R 2009 *Phys. Rev. Lett.* **103** 060402
[43] Tsatsos M C, Nguyen J H V, Lode A U J, Telles G D, Luo D, Bagnato V S and Hulet R G 2017 arXiv:1707.04055
[44] Lode A U J, Streltsov A I, Sakmann K, Alon O E and Cederbaum L S 2012 *Proc. Natl Acad. Sci. USA* **109** 13521
[45] Brezinova I, Lode A U J, Streltsov A I, Alon O E, Cederbaum L S and Burgdörfer J 2012 *Phys. Rev.* A **86** 013630
[46] Lode A U J, Klaiman S, Alon O E, Streltsov A I and Cederbaum L S 2014 *Phys. Rev.* A **89** 053620
[47] Brezinova I, Lode A U J, Streltsov A I, Cederbaum L S, Alon O E, Collins L A, Schneider B I and Burgdörfer J 2014 *J. Phys.: Conf. Ser.* **488** 012032
[48] Klaiman S, Lode A U J, Streltsov A I, Cederbaum L S and Alon O E 2014 *Phys. Rev.* A **90** 043620
[49] Weiner S E, Tsatsos M C, Cederbaum L S and Lode A U J 2017 *Sci Rep.* **7** 40122
[50] Tsatsos M C and Lode A U J 2015 *J. Low. Temp. Phys.* **181** 171
[51] Lode A U J, Chakrabarti B and Kota V K B 2015 *Phys. Rev.* A **92** 033622
[52] Fischer U R, Lode A U J and Chatterjee B 2015 *Phys. Rev.* A **91** 063621
[53] Lode A U J and Bruder C 2016 *Phys. Rev.* A **94** 013616
[54] Roy R, Gammal A, Tsatsos M C, Chatterjee B, Chakrabarti B and Lode A U J 2018 *Phys. Rev.* A **97** 043625
[55] Dutta S, Tsatsos M C, Basu S and Lode A U J 2018 arXiv:1802.02407
[56] Mueller E J, Ho T-L, Ueda M and Baym G 2006 *Phys. Rev.* A **74** 033612
[57] Müstecaplıoğlu O E, Zhang M, Yi S, You L and Sun C P 2003 *Phys. Rev.* A **68** 063616
[58] Song S-W, Zhang Y-C, Zhao H, Wang X and Liu W-M 2014 *Phys. Rev.* A **89** 063613
[59] Ho T-L and Yip S K 2000 *Phys. Rev. Lett.* **84** 4031
[60] Mivehvar F, Piazza F and Ritsch H 2017 *Phys. Rev. Lett.* **119** 063602
[61] Alon O E, Streltsov A I and Cederbaum L S 2008 *Phys. Rev.* A **77** 033613
[62] Fasshauer E and Lode A U J 2016 *Phys. Rev.* A **93** 033635
[63] Lode A U J, Tsatsos M C, Fasshauer E, Lin R, Papariello L, Molignini P and Lévêque C 2018 MCTDH-X: The time-dependent multiconfigurational Hartree for indistinguishable particles software http://ultracold.org
[64] Lode A U J, Sakmann K, Alon O E, Cederbaum L S and Streltsov A I 2012 *Phys. Rev.* A **86** 063606
[65] Lode A U J 2015 Tunneling dynamics in open ultracold bosonic systems *Springer Theses* Springer, Heidelberg
[66] Sakmann K 2011 Many-body Schrödinger dynamics of Bose–Einstein condensates *Springer Theses* Springer, Heidelberg
[67] Olshanii M 1998 *Phys. Rev. Lett.* **81** 938
[68] Wagner A, Nunnenkamp A and Bruder C 2012 *Phys. Rev.* A **86** 023624
[69] Bloch I 2008 *Nature* **453** 1016
[70] Jaksch D, Briegel H J, Cirac J I, Gardiner C W and Zoller P 1999 *Phys. Rev. Lett.* **82** 1975
[71] Mandel O *et al* 2003 *Nature* **425** 937
[72] Briegel H J and Raussendorf R 2001 *Phys. Rev. Lett.* **86** 910
[73] Raussendorf R and Briegel H J 2001 *Phys. Rev. Lett.* **86** 5188
[74] Raussendorf R and Briegel H J 2002 *Quantum Inf. Comput.* **2** 443
[75] Walther P *et al* 2005 *Nature* **434** 169
[76] Kiesel N *et al* 2005 *Phys. Rev. Lett.* **95** 210502
[77] Cramer M, Bernard A, Fabbri N, Fallani L, Fort C, Rosi S, Caruso F, Inguscio M and Plenio M B 2013 *Nat. Commun.* **4** 2161
[78] Léonard J, Morales A, Zupancic P, Esslinger T and Donner T 2017 *Nature* **543** 87
[79] Léonard J, Morales A, Zupancic P, Esslinger T and Donner T 2017 arXiv:1711.07988
[80] Mivehvar F, Ritsch H and Piazza F 2017 *Phys. Rev. Lett.* **118** 073602
[81] Exl L 2017 *Comput. Phys. Commun.* **221** 352
[82] Exl L, Mauser N J and Zhang Y 2016 *J. Comput. Phys.* **327** 629